



# Insect nephrocyte function is regulated by a store operated calcium entry mechanism controlling endocytosis and Amnionless turnover

Shruthi Sivakumar<sup>a,1</sup>, Sara Miellet<sup>b,c,1</sup>, Charlotte Clarke<sup>a</sup>, Paul S. Hartley<sup>a,\*</sup>

<sup>a</sup> Department of Life and Environmental Sciences, Faculty of Science and Technology, Bournemouth University, Dorset BH12 5BB, UK

<sup>b</sup> Illawarra Health and Medical Research Institute, Wollongong, NSW, Australia

<sup>c</sup> Molecular Horizons, University of Wollongong, NSW, Australia

## ARTICLE INFO

### Keywords:

*Drosophila*  
Circulation  
Nephrocytes  
Signalling  
Calcium

## ABSTRACT

Insect nephrocytes are ultrafiltration cells that remove circulating proteins and exogenous toxins from the haemolymph. Experimental disruption of nephrocyte development or function leads to systemic impairment of insect physiology as evidenced by cardiomyopathy, chronic activation of immune signalling and shortening of lifespan. The genetic and structural basis of the nephrocyte's ultrafiltration mechanism is conserved between arthropods and mammals, making them an attractive model for studying human renal function and systemic clearance mechanisms in general. Although dynamic changes to intracellular calcium are fundamental to the function of many cell types, there are currently no studies of intracellular calcium signalling in nephrocytes.

In this work we aimed to characterise calcium signalling in the pericardial nephrocytes of *Drosophila melanogaster*. To achieve this, a genetically encoded calcium reporter (GCaMP6) was expressed in nephrocytes to monitor intracellular calcium both *in vivo* within larvae and *in vitro* within dissected adults. Larval nephrocytes exhibited stochastically timed calcium waves. A calcium signal could be initiated in preparations of adult nephrocytes and abolished by EGTA, or the store operated calcium entry (SOCE) blocker 2-APB, as well as RNAi mediated knockdown of the SOCE genes *Stim* and *Orai*. Neither the presence of calcium-free buffer nor EGTA affected the binding of the endocytic cargo albumin to nephrocytes but they did impair the subsequent accumulation of albumin within nephrocytes. Pre-treatment with EGTA, calcium-free buffer or 2-APB led to significantly reduced albumin binding. Knock-down of *Stim* and *Orai* was non-lethal, caused an increase to nephrocyte size and reduced albumin binding, reduced the abundance of the endocytic cargo receptor Amnionless and disrupted the localisation of Dumbfounded at the filtration slit diaphragm.

These data indicate that pericardial nephrocytes exhibit stochastically timed calcium waves *in vivo* and that SOCE mediates the localisation of the endocytic co-receptor Amnionless. Identifying the signals both up and downstream of SOCE may highlight mechanisms relevant to the renal and excretory functions of a broad range of species, including humans.

## 1. Introduction

Nephrocytes are haemolymph ultrafiltration cells found in a wide range of arthropod species. Initially identified by their ability to rapidly accumulate injected tracer dyes, recent research has established that nephrocytes play a central role in immunity, organ homeostasis and regulation of lifespan (Kowalevsky, 1886; Troha et al., 2019; Hartley et al., 2016). Nephrocytes exhibit exceptional levels of endocytosis and possess filtration slit diaphragms close to their surface which limits the size of molecules the nephrocytes endocytose (Crossley, 1972). These

two aspects of their biology appear ancestral to mammalian kidney function (Denholm and Skaer, 2009). Both the genetics of endocytosis and filtration diaphragm formation are conserved between arthropods and mammals and the nephrocytes of the fruit fly *Drosophila melanogaster* have become a highly tractable model with which to study aspects of human renal function (Weavers et al., 2009; Zhuang et al., 2009; Helmstädter and Simons, 2017). Additionally, nephrocytes accumulate, and are affected by, environmental xenotoxins, suggesting that these cells may buffer or modify the impact of ecologically important pollutants (Domingues et al., 2017; Abdalla et al., 2015). As such, studies of

\* Corresponding author.

E-mail address: [phartley@bournemouth.ac.uk](mailto:phartley@bournemouth.ac.uk) (P.S. Hartley).

<sup>1</sup> These authors contributed equally to the work.

nephrocytes are contributing to our understanding of basic cell biology, biomedical science and ecology.

Nephrocytes in *Drosophila melanogaster* appear to exist as two anatomically distinct populations with similar function but independent developmental trajectories. The first population to develop are the Garland cells close to the developing oesophagus which differentiate into functional nephrocytes during embryogenesis. The second population to develop are the pericardial nephrocytes which proliferate during embryogenesis as part of the heart's development and then differentiate during the L1-L3 larval stages. The differentiation and viability of both nephrocyte populations requires expression of *dKlf15* (Ivy et al., 2015), and both are functionally stable during metamorphosis. Throughout development and adulthood the Garland cells remain adjacent to the oesophagus and the pericardial nephrocytes remain adjacent to the beating heart. This developmental stability means that the effects of exogenous environmental and genetic factors on nephrocytes may be carried forward from embryogenesis until the organism's death.

Gaining an understanding of the signalling mechanisms regulating nephrocyte function yields important information about the factors controlling ultrafiltration and clearance in a wide range of species and different research contexts. Conserved roles in nephrocyte endocytosis and filtration diaphragm maintenance have been demonstrated for several signalling pathways, including the conserved src kinase Src64B (Tutor et al., 2014); Shaggy (an ortholog of mammalian GSK3) which has relevance to diabetic nephropathy (Hurcombe et al., 2019); Skittles, a phosphatidylinositol (Crossley, 1972)-phosphate 5-kinase (Gass et al., 2022), and Rap1 which signals downstream of the slit diaphragm protein Nephrin (Maywald et al., 2022). However, there have been no studies of calcium signalling in insect nephrocytes and, more broadly, there are open questions as to whether nephrocyte function is constitutive, or whether there is a level of functional dynamism and responsiveness. Mammalian models have demonstrated that calcium signalling within cell types analogous to nephrocytes is linked to their function. For example it has been demonstrated that calcium signalling in rat proximal renal tubules is dynamically linked with pathology (Szebenyi et al., 2015), that calcium waves occur in murine podocytes and are modified by renal injury (Burford et al., 2014), and that store operated calcium entry (SOCE) is crucial for reabsorption of albumin via a mechanism linking the endocytic coreceptor Amnionless with the SOCE channel Orai1 (Zeng et al., 2017). Considering the importance of calcium signalling in the mammalian kidney and the high conservation of the SOCE mechanism, it was predicted that SOCE may contribute to nephrocyte function in insect nephrocytes.

In this work, calcium dynamics were recorded in nephrocytes expressing a genetically encoded calcium reporter (GCaMP6, (Chen et al., 2013), in conjunction with imaging of larval nephrocytes *in vivo*, as well as nephrocytes in semi-intact adult abdominal preparations. Calcium signals were modified by pharmacological means, as well as genetic knock down of genes comprising key components of the SOCE mechanism, *Orai* and *Stim*. Nephrocyte function was then assessed by endocytic uptake assays and confocal microscopic imaging of Amnionless, a coreceptor in the endocytic receptor CUBAM complex (Larsen et al., 2018; Atienza-Manuel et al., 2021), as well as imaging of Dumbfounded, an ortholog of the mammalian slit diaphragm protein KIRREL/NEPH1 (Ruiz-Gómez et al., 2000). The data define for the first time that dynamic calcium signalling events occur in insect nephrocytes and that these signals are linked to nephrocyte function. A discussion is then presented regarding the physiological relevance of calcium signalling in insect nephrocytes with specific focus on how this relates to excretory and clearance function in general.

## 2. Methods

### 2.1. Chemicals and *Drosophila* strains used in this study

All stock chemicals were from Sigma-Aldrich (Dorset, UK), whereas

all fluorescently conjugated stains were from Invitrogen (Thermo Fisher, UK). anti-Dumbfounded antibodies were raised in rabbits to a synthetic polypeptide corresponding to amino acids 32–46 (KSKKNKSSQSSHHGD; Cambridge Research Biochemicals, Cleveland, UK). Antisera to Amnionless were described in (Ivy et al., 2015). Flies were reared at 25°C on a standard cornmeal-yeast-agar diet under 12 h:12 h light:dark cycles. *Drosophila* stocks were: *Dorothy-Gal4*, *UAS-GCaMP6<sup>Medium</sup>* (Bloomington #42748), *UAS-Orai* RNAi (Bloomington #53333, which expresses RNAi of *Orai* (*olf186-F*) under UAS control in the VALIUM20 vector), two independent *UAS-Stim* RNAi lines (Bloomington #27263, which expresses RNAi of *Stim* under UAS control in the VALIUM10 vector and stock #51685, which expresses RNAi of *Stim* under UAS control in the VALIUM22 vector).

### 2.2. *In vivo* imaging of intra-nephrocyte calcium in larvae

Preliminary experiments indicated that the calcium signal from pericardial nephrocytes was easily recorded using flies where *GCaMP6<sup>Medium</sup>* (Chen et al., 2013) was driven by *Dorothy-Gal4*. Whilst *Dorothy-Gal4* expresses in nephrocytes it also drives expression of genes in the midgut and haemocytes, neither of which affected nor interfered with the recording of GCaMP6 fluorescence in pericardial nephrocytes. Two imaging methods were developed, the first was *in vivo* recording from immobilised larvae, whereas the second method relied on the use of adult pericardial nephrocytes in semi-intact abdominal preparations. To record GCaMP6 fluorescence from larvae nephrocytes, larvae were anaesthetised by exposure to triethylamine (50 % triethylamine in 25 % ethanol, 25 % distilled water) for approximately 10 min. Larvae were then mounted onto a glass microscope slide between two stacks of No.1 coverslips, each stack comprising three coverslips. A final coverslip was placed on top of the larva. This set-up was adequate to gently compress the larva to allow visualisation of the pericardial cells and beating dorsal vessel. Larval preparations were visualised using a Zeiss AxioLab A1 LED fluorescence microscope fitted with a 10x objective and a Ximea QiD 12 MB high sensitivity camera. Recordings were collected at a frame rate of up to 25 frames per second depending on the experimental timeframe, using proprietary image collection software (CamTool). Images were collected using an 8-bit grey scale (255greys) and camera settings were chosen to obtain signals not exceeding the 255th grey scale.

## 3. Live imaging of intra-nephrocyte calcium in semi-intact abdominal preparations

The second method utilised adult flies which were dissected to reveal the dorsal vessel and pericardial nephrocytes (a methodology developed to analyse cardiac and nephrocyte function and described in detail by Ocorr et al. (2009). This was done in a 30 mm diameter plastic petri dish, in calcium and magnesium-free Hanks Basic Saline (HBSS). After rinsing preparations with calcium-free HBSS, 3 mL of calcium-free HBSS was added to the dish and the dish was placed on a Zeiss AxioLab A1 LED microscope stage, with a 10x water-dipping objective focused on the pericardial nephrocytes. Video recordings were obtained as described for larval imaging. To initiate calcium transients, 1 mL of 'initiation buffer' (10 mM CaCl<sub>2</sub> in HBSS, to a final concentration of 2.5 mM) was added to the dish. In some experiments the dissection buffer or initiation buffer or both buffers also included pharmacological agents, as reported in the figures. Baseline fluorescence was recorded (as described above), for 10 s before addition of induction buffer.

## 4. Quantification of calcium signals

The calcium signal for several nephrocytes per fly were analysed using ImageJ (Schneider et al., 2012). Briefly, the image sequence was opened as a virtual stack and a region of interest placed over individual nephrocytes, ensuring that the nephrocyte remained within the ROI during the entire timeframe of the image sequence (care was needed to

avoid losing signal beyond the ROI during heart contractions, which move the nephrocytes) and the ROI did not overlap other nephrocytes. The maximum fluorescence signal in the region of interest was recorded using the 'multimeasure' plugin for every frame and transferred to a Microsoft Excel spreadsheet. Background fluorescence (F0) was established by averaging the maximum fluorescence signal from nephrocytes in the first 200 frames prior to the addition of calcium or other reagents, and then dividing the subsequent fluorescence increase (F1) by this figure and expressing changes as the ratio of F1/F0.

## 5. Nephrocyte albumin uptake, staining and confocal imaging

Adult nephrocytes were exposed in semi-intact abdominal dissections in the presence of HBSS (CaCl<sub>2</sub> at 1.7 mM) and incubated with fluorescently conjugated albumin (5 µg/mL) at 4°C for 5 min. Unbound albumin cargo was washed off by rinsing the preparation three times using 4°C HBSS. Cells were fixed at this stage to assess albumin binding using 3.8 % formaldehyde in HBSS at 4°C for 10 min, or incubated in HBSS (20°C) for 20 min to assess albumin endocytosis and then fixed. Fixed nephrocytes were then counter-stained overnight at 4°C with wheatgerm agglutinin (WGA) or antisera to Amnionless (1:100) or Dumbfounded (1:100). Imaging was performed using a Lecia SP8 confocal microscope coupled to proprietary software (LAS X). Typically, confocal slices were obtained for stained cells and where relevant, Z-projections prepared in ImageJ using the same number of stacks for each image. Image modification was done equally to all data and was limited to colour application, as well as modulation of contrast and brightness.

## 6. Statistics

Graphs were prepared in Microsoft Excel and statistics were tested using VassarStat (<https://vassarstats.net/>). A Shapiro Wilk test was used to assess whether data was normally distributed. Two means were compared using a student's *t*-test, whereas more than two means were compared using 1-Way ANOVA, with a post-hoc Tukey's Test. Statistical significance was accepted when  $P < 0.01$ . Graphs depict the mean  $\pm$  standard error of the mean ( $\pm$ SEM).

## 7. Results

### 7.1. Stochastic calcium waves in larval pericardial nephrocytes

The growth and differentiation of pericardial nephrocytes occurs rapidly between the L1 and L3 stages and, from functional data, it is assumed the cells are terminally differentiated by the L3 stage (Ivy et al., 2015). At the L3 stage, pericardial nephrocytes can be identified through the dorsal cuticle based on their morphology and anatomical location adjacent to the beating dorsal vessel. Using anaesthetised L3 stage larvae expressing *GCaMP6* under the control of *Dorothy-Gal4*, it was possible to identify brief, transient increases in fluorescence emanating from the pericardial nephrocytes. Image capture was hampered by the myogenic activity of the heart, which shifted the position of pericardial nephrocytes considerably during imaging. However, when viewed over time, it was possible to quantify calcium transients from their initiation to completion in the larval pericardial nephrocyte population (refer to the time-lapse footage (3x speed) of the distal region of an L3 larva in Fig. S1 (the first calcium signal starts in a nephrocyte at the bottom left of the footage at ~3 s); and (1x speed) footage of an individual nephrocyte in Fig. S2).

An individual nephrocyte would initiate a calcium transient at a single discrete region of the cell (Fig. 1A), the signal would then increase throughout the nephrocyte as a wave and dissipate. These signals were the only type observed and were termed intracellular calcium waves (ICWs). Within individual nephrocytes there were irregular intervals between ICWs and over a ten-minute recording period, a single nephrocyte might exhibit a maximum of two or three ICWs. Although in most cases some of the pericardial nephrocytes were partially obscured by the fat body or trachea, ICWs never occurred synchronously within the pericardial nephrocyte population (Fig. 1B), nor was there any evidence that two, or more nephrocytes signalled coincidentally. Typically, the waves were observed in a maximum of three or four nephrocytes at a time, with no sense of any spatial patterning to the waves within the nephrocyte population. There was no consistency between where in the nephrocyte population the waves initiated and propagated (i.e. ICWs did not start in anterior nephrocytes and then move to posterior nephrocytes, or *vice versa*). Where a second or third ICW initiated in a nephrocyte, it initiated at a different locality to the first (an example provided in Fig. 1A).

By averaging individual ICWs from several experimental recordings,

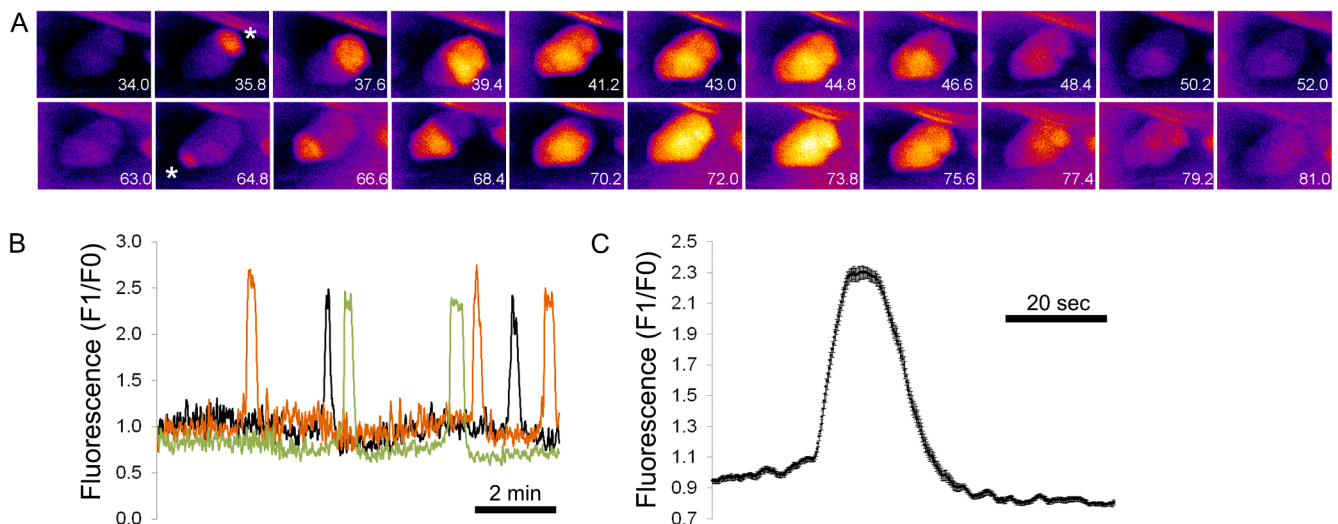


**Fig. 1.** Stochastic *in vivo* calcium waves in *Drosophila* pericardial nephrocytes. Live *Drosophila* expressing *GCaMP6* in pericardial nephrocytes under the control of *Dot-Gal4* were imaged through the cuticle at the L3 larval stage. (A) The micrographs show an example of two consecutive calcium waves initiating at different sites in the same nephrocyte (asterisks); the timestamp of the frame (in seconds) is shown. (B) Example traces of endogenous (*in vivo*) calcium transients in three different L3 nephrocytes. (C) The graph shows mean fluorescence traces (F1/F0,  $\pm$ SEM) from nephrocytes within two independent larvae;  $n = 17$  nephrocytes.

it was established that their baseline-to-baseline period was  $18.6 (\pm 0.9)$  seconds and the time from baseline-to-peak signal was  $3.9 (\pm 0.4)$  seconds (Fig. 1C). The propagation velocity of the waves was  $3.8 \mu\text{m}$  per second ( $\pm 0.4 \mu\text{m}$  per second,  $n = 10$  waves). These data established that insect pericardial nephrocytes repeatedly initiate ICWs *in vivo*, however these waves occur with a stochastic frequency within the population, rather than synchronously or with any predictable frequency.

## 8. Calcium *in vitro*

Whilst the imaging of larval nephrocytes was instructive about qualitative aspects of calcium waves in pericardial nephrocytes, a more tractable system was developed using adult semi-intact abdomen preparations. When pericardial nephrocytes were dissected in calcium-free buffer and then initiation buffer added (HBSS with 10 mM  $\text{CaCl}_2$ , to a final concentration of 2.5 mM), a robust increase in GCaMP6 fluorescence was observed, simultaneously in all the pericardial nephrocytes (Fig. 2A).

Several minutes after this initial synchronous calcium wave, there were occasional asynchronous ICWs in nephrocytes, similar to those seen *in vivo* (Fig. 2B) but these were rare (<3 over a period of one hour), making their quantification very challenging. Despite this limitation it was possible to characterise the calcium entry into nephrocytes pharmacologically using the Orai-channel blocking agent 2-APB or the calcium chelator EGTA. Nephrocytes pre-incubated with either agent displayed no GCaMP6 signal upon addition of initiation buffer (Fig. 2C and 2D;  $P < 0.001$ ).

## 9. Effect of calcium depletion on nephrocyte endocytic function

Given that ICWs were recorded in larval and adult nephrocytes and these waves could be abolished by pharmacological means, it was hypothesised that modulation of calcium entry may be linked with nephrocyte endocytic function. To test this possibility nephrocytes in adult abdominal preparations were incubated with fluorescently labelled albumin in the presence of control buffer replete with calcium, or buffers without calcium, or containing 10 mM EGTA or 100  $\mu\text{M}$  2-APB (Fig. 3).

In 'pulse-chase' experiments, nephrocytes were incubated with albumin at  $4^\circ$  for 5 min to allow for binding, rinsed and imaged in order to quantify binding. Then endocytosis was allowed to proceed for 20 min at  $20^\circ\text{C}$  and the cells were fixed and imaged after counterstaining. In controls, albumin accumulated within discrete inclusions (presumed to be early endosomes) close to the nephrocytes' plasma membrane (Fig. 3A-D). In contrast, when adding the calcium chelator EGTA (Fig. 3E-F), fewer inclusions were present, and albumin appeared to accumulate within the nephrocytes' labyrinthine channels (compare Fig. 3D and 3H). This qualitative difference to the location of albumin was not due to quantitative differences to the initial amount of albumin binding the nephrocytes in the respective buffers, (Fig. 3I,  $P > 0.05$ ). However, when nephrocytes were pre-treated for one hour with Ca-free HBSS, EGTA or 2-APB before allowing albumin to bind, the resulting albumin binding signal was significantly reduced (an example is presented for 2-APB in Fig. 3J and 3K and quantified data are presented in Fig. 3L;  $P < 0.01$ ).

Given that endocytosis by nephrocytes is reliant on the endocytic co-receptor Amnionless, it was reasoned that the albumin result may correlate with a change to the location of Amnionless. To address this, Amnionless was assessed after the one-hour treatment of nephrocytes with either EGTA or 2-APB and found to have increased within the nephrocytes, especially within the cortex (Fig. 3M & 3N), consistent with calcium influx being required to maintain Amnionless turnover. In contrast, the pre-treatment with either EGTA or 2-APB had little to no effect on Dumbfounded staining, which remained constant, both in terms of signal quality and intensity (Fig. 3O & 3P;  $P > 0.05$ ).

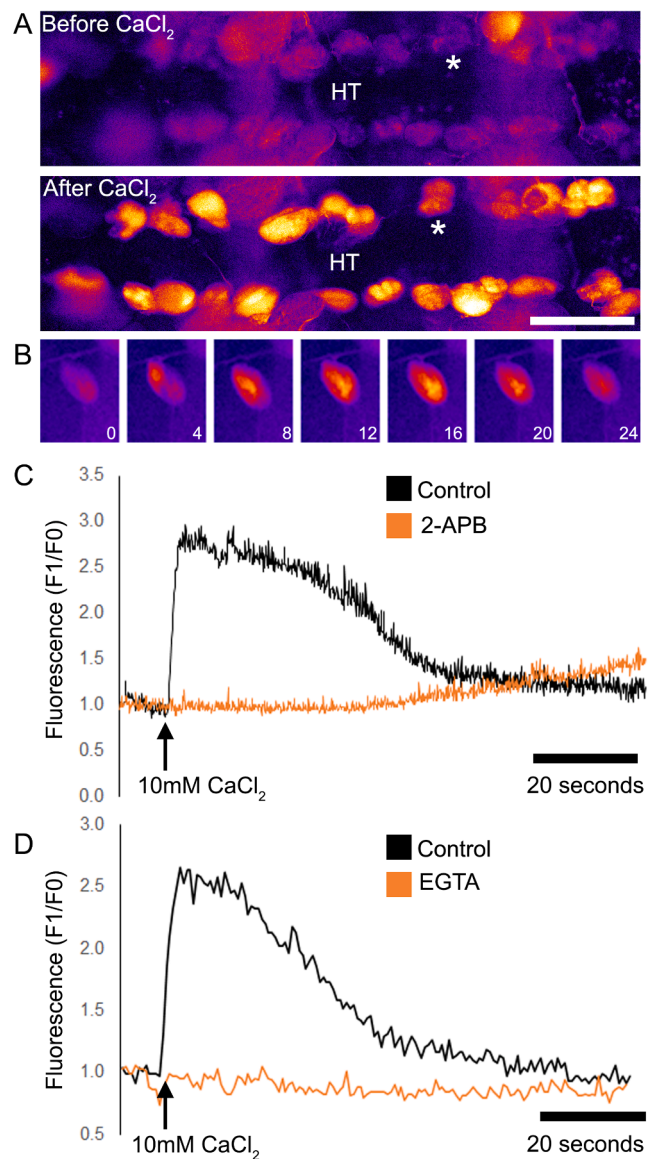


**Fig. 2.** 2-APB and EGTA prevents calcium entry into pericardial nephrocytes. Flies expressing the calcium reporter *GCaMP6* in nephrocytes under the control of *Dot-Gal4* were imaged in semi-intact 1-week old adult abdomen preparations. (A) Video-micrographs of nephrocyte fluorescence (false coloured) before and after the addition of a bolus of 'initiation buffer' (10 mM  $\text{CaCl}_2$ , to a final concentration of 2.5 mM); scale bar = 100  $\mu\text{m}$ ; the asterisk identifies the same individual nephrocyte. (B) Video stills of a single intracellular calcium wave propagating across a nephrocyte; time in seconds is shown. (C & D) Traces show the relative increase in the GCaMP6 fluorescence signal and the impact of 100  $\mu\text{M}$  2-APB and 10 mM EGTA, respectively.

### 9.1. *Stim* and *Orai* mediate calcium entry and endocytic function of pericardial nephrocytes

Calcium influx can be initiated by release of calcium from internal stores activating *Stim* in the endoplasmic reticulum, which then facilitates the opening of the plasma membrane calcium channel encoded by *Orai* (reviewed in (Johnson et al., 2022)). Mammalian *Orai1* has recently been implicated in the regulation of albumin uptake by mammalian renal proximal tubule cells (Zeng et al., 2017). Therefore, in order to complement the experiments where the effect of short-term calcium modulation was examined, the genetic components of SOCE were silenced by crossing the *GCaMP6*-expressing flies with RNAi lines corresponding to either *Orai* or *Stim*. Whilst RNAi lines did not affect

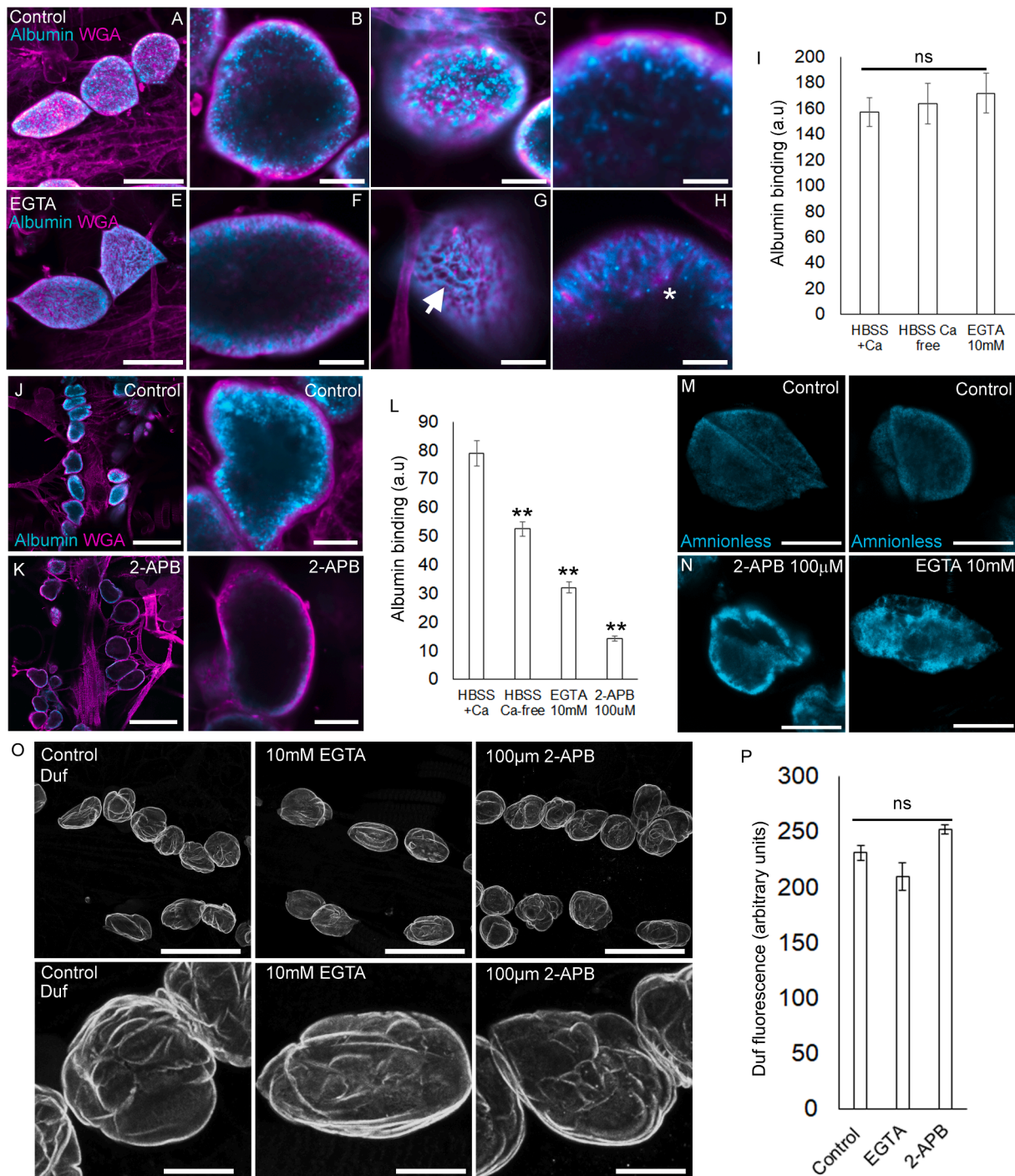


**Fig. 3.** Calcium entry is required for albumin endocytosis and Amnionless localisation. (A-H) Confocal images of adult pericardial nephrocytes incubated briefly with albumin (cyan) at 4°C for 5 min and then imaged after endocytosis was allowed to proceed for 30 min in calcium-replete HBSS (A-D) or EGTA 10 mM (E-H). Cells were fixed and counterstained with wheatgerm agglutinin (WGA, magenta). (A & E) Confocal Z-projections; scale bars = 50  $\mu$ m. (B & F) Single confocal section of nephrocyte midpoint; scale bar = 15  $\mu$ m. (C & G) Single confocal section of nephrocyte surface; scale bar = 5  $\mu$ m. (D & H) Confocal cross section of the nephrocyte midpoint, scale bar = 5  $\mu$ m. Arrow denotes lack of albumin puncta; asterisk denote area of signal retention in labyrinthine channels. (I) Quantification of albumin binding after binding at 4°C for 5 min in the presence of the respective buffer.  $n = 49-62$  nephrocytes from four or five different individual flies; ns = not significantly different to control. (J & K) Confocal images of albumin binding to pericardial nephrocytes after one hour of pre-treatment with either control buffer or 100  $\mu$ M 2-APB. Images show low magnification of nephrocytes (left, scale bars = 100  $\mu$ m) and a representative single nephrocyte (right, scale bars = 15  $\mu$ m). (L) Quantification of albumin binding after pre-treatment for 1 h with control buffer (HBSS with calcium), calcium free HBSS, 10 mM EGTA or 100  $\mu$ M 2-APB.  $n = 49-62$  nephrocytes from 5 individual flies; \*\* $P < 0.01$  compared to control buffer. (M & N) Confocal images of control (M) and 2-APB or EGTA-treated nephrocytes (N) stained for Amnionless; scale bar = 20  $\mu$ m. (O) Confocal Z-stacks of Dumbfounded staining after pre-treatment with 10 mM EGTA or 100  $\mu$ M 2-APB for 30 min; upper and lower scale bars = 100  $\mu$ m and 20  $\mu$ m, respectively. (P) Quantification of Duf immunofluorescence signal on nephrocytes treated with 10 mM EGTA or 100  $\mu$ M 2-APB. ns = not statistically significant by 1-Way ANOVA. (For interpretation of the references to colour in this figure legend, the reader is referred to the web version of this article.)

nephrocyte numbers ( $25.4 \pm 0.8$ ;  $26.5 \pm 0.7$  and  $24.8 \pm 0.6$  nephrocytes for control, *Orai* knockdown and *Stim* knockdown, respectively;  $P > 0.05$ ; Fig. 4A), they caused a small yet significant increase to nephrocyte size (Fig. 4B). Importantly, RNAi lines abolished the GCaMP6 fluorescence signal upon addition of initiation buffer compared to controls (Fig. 4C, D and E). Next, the consequence of *Stim* and *Orai* RNAi on the nephrocytes' endocytic function was assessed using albumin (Fig. 5). Whilst albumin binding at 4°C was equivalent between genotypes, when nephrocytes were transferred to 20°C the albumin signal remained within the labyrinthine channels near the surface of nephrocytes in which *Stim* or *Orai* had been knocked-down (Fig. 5), a phenotype similar to that seen when calcium entry had been blocked by EGTA.

## 9.2. Impact of *Stim* or *Orai* knockdown on *Amnionless* and *Dumbfounded*

Given the albumin uptake in *Stim* or *Orai* knock-down nephrocytes was abnormal, it was assumed this may be a result of changes to the localisation of the endocytic receptor *Amnionless* at the nephrocyte surface. *Amnionless* expression levels at the nephrocyte surface were  $98.3 (\pm 3.8 \text{ au})$ ,  $63.2 (\pm 2.1 \text{ au})$  and  $60.6 (\pm 2.3 \text{ au})$  for control, *Orai* or *Stim* knockdown, respectively ( $P < 0.01$ , Fig. 6), indicating that components of the SOCE mechanism help maintain the turnover of *Amnionless*. However, where EGTA or 2-APB pre-treatment had increased the *Amnionless* signal, the longer-term RNAi mediated knockdown of *Stim* or *Orai* had caused the *Amnionless* signal to decrease. In addition, the localisation of the slit diaphragm protein *Dumbfounded* (*Duf*) was also assessed and found to be slightly decreased in terms of overall signal in both *Stim* or *Orai* knock-down nephrocytes (Fig. 7,  $P < 0.01$ ) and qualitatively affected at the surface where *Duf* appeared to form abnormal 'ruffles' on the nephrocyte membrane. These data indicate that *Stim* and *Orai* mediate the localisation of *Amnionless*, as well as *Duf* in nephrocytes.

## 10. Discussion

The insect nephrocyte has become an important model for understanding how clearance of molecules from circulating fluids maintains organism homeostasis. There is now extensive evidence supporting the hypothesis that the molecular genetics underpinning the function of insect nephrocytes is evolutionarily conserved across a diverse range of species, from arthropods to mammals. In this work we demonstrate for the first time that nephrocytes exhibit stochastic calcium waves *in vivo* and established that key aspects of nephrocyte function are linked to calcium signalling via a *Stim* and *Orai*-dependent SOCE mechanism controlling *Amnionless*. This study emphasises that nephrocyte signalling biology is far more dynamic than previously thought and highlights *Drosophila* as a means of studying calcium-dependent aspects of haemolymph filtration and circulatory clearance mechanisms in general. These observations are important because of the broad biomedical and ecological significance of nephrocytes and calcium signalling, which can be addressed using a simple and highly tractable *Drosophila* model.

Intracellular calcium waves (ICWs) are known to occur in a diverse range of cell types and species, where they range from 'fast' (3–30  $\mu\text{m/s}$ ) to 'slow' (0.2–2.0  $\mu\text{m/s}$ ) according to the speed they propagate across a cell (Jaffe, 2008). In the current work the ICWs propagated from a single point, across a nephrocyte at approximately 3.8  $\mu\text{m/s}$ , which represents a 'fast' wave, albeit at the lower end of the range, as suggested by Jaffe (Jaffe, 2010). It should be noted that some researchers use the term 'slow' and 'fast' to describe the relative differences in ICW velocity recorded in the same cell type under different conditions, e.g. HeLa cells (Li et al., 2018), where the velocity we observed would be regarded as a 'slow' wave. The *in vivo* recording of larval *Drosophila* pericardial nephrocytes demonstrated that ICWs would initiate in individual nephrocytes and that a stochastic pattern of incidence existed within the population because there was neither a predictability to the timing of the ICWs, nor any apparent synchrony or spatial patterning within the nephrocyte population. ICWs appeared to initiate at a single locus and then propagate across a cell. Where consecutive ICWs were observed in

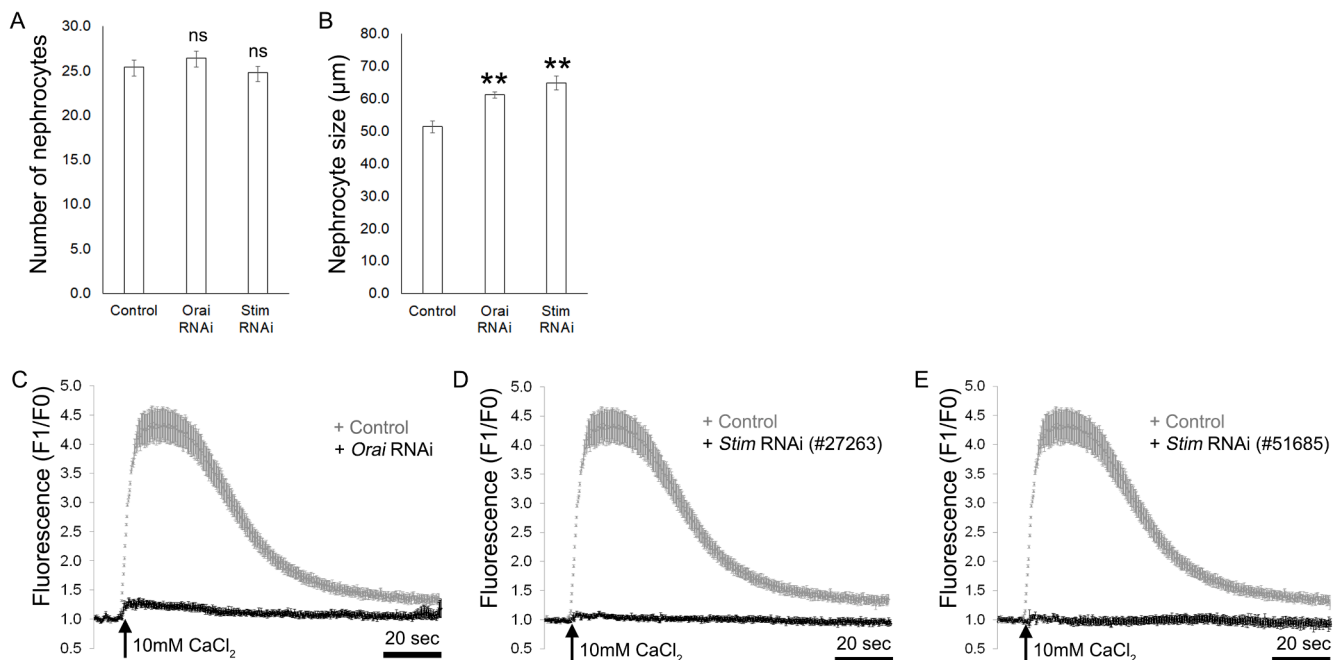


**Fig. 4.** Impact of *Orai* or *Stim* RNAi on pericardial nephrocytes. Nephrocyte numbers in adult flies of the stated genotypes, ns = not significantly different from control (*Dot-Gal4* out-crossed to *w<sup>1118</sup>*);  $n = 12\text{--}13$  flies for each genotype. (B) Pericardial nephrocyte sizes in flies where *Orai* or *Stim* were silenced under the control of *Dot-Gal4*. Control is *w<sup>1118</sup>* outcrossed to the *Dot-Gal4* driver line;  $n = 18\text{--}19$  nephrocytes from three different individual flies;  $**P < 0.01$  compared to control. (C, D, E) Graphs show the mean ( $\pm$ SEM) change in fluorescence from baseline ( $F1/F0$ ) in nephrocytes expressing *GCaMP6* under the control of *Dot-Gal4* (Control), *UAS-Orai* RNAi or two independent *UAS-Stim* RNAi lines.

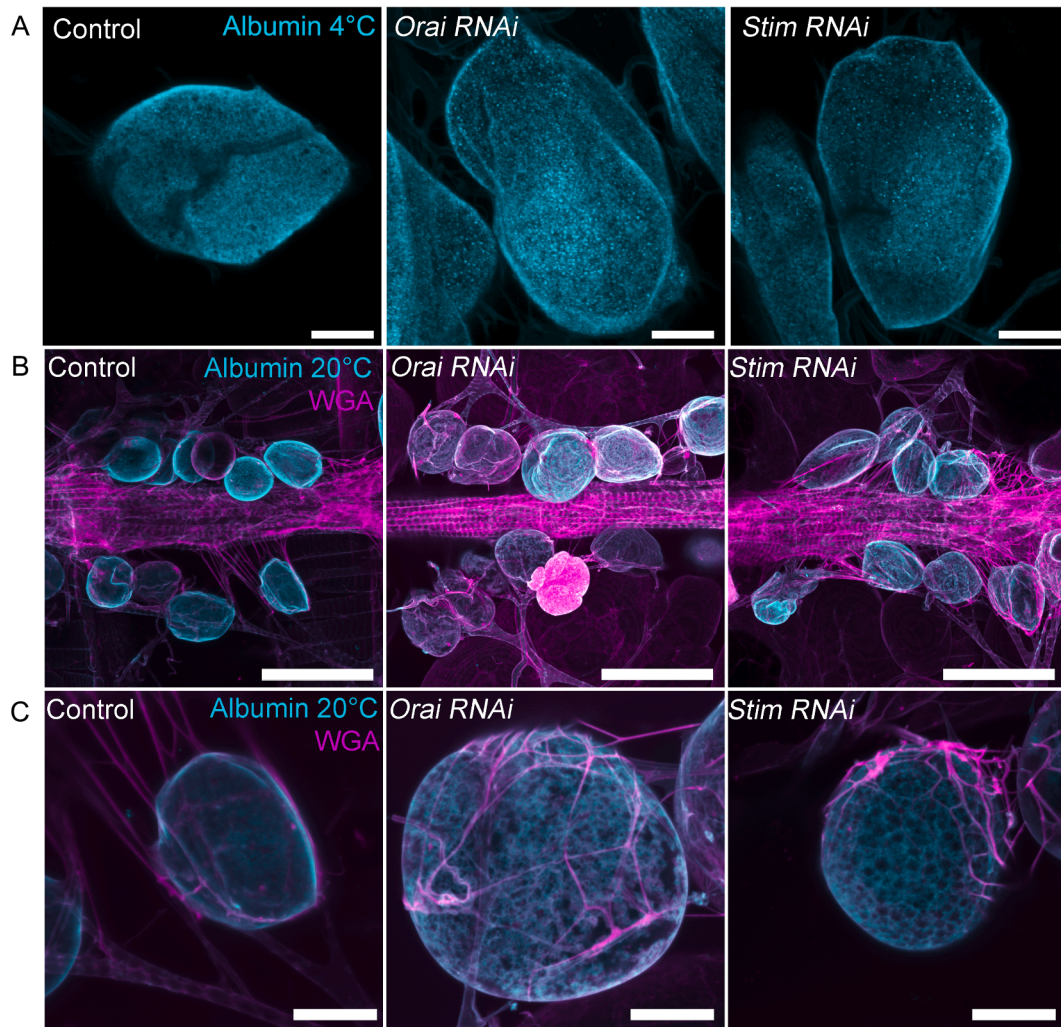


**Fig. 5.** Silencing *Orai* or *Stim* disrupts albumin endocytosis by nephrocytes. The micrographs show z-projections of confocal stacks through nephrocytes that were fixed after 5 min at 4°C in the presence of fluorescently labelled albumin; scale bar = 10 μm (B) Images show a low magnification of the heart, with the pericardial nephrocytes' albumin signal after 20 min at 20°C; scale bar = 100 μm. (C) Higher magnification confocal z-projections of the albumin signal within nephrocytes that had endocytosed albumin for 20 min at 20°C; scale bar = 25 μm.

the same nephrocyte, there was evidence of initiation at different locations, suggesting that multiple Endoplasmic reticulum-plasma membrane nanodomains may exist in nephrocytes. How a wave is initiated in nephrocytes is unclear but there has been extensive modelling in other cell types demonstrating that subcellular calcium sparks couple with 'calcium release units' which culminate in the triggering of a wave (Nivala et al., 2013). Calcium sparks were not recorded using either the *in vivo* or *in vitro* imaging methodology in this study. Additionally, it was not possible with the imaging system we used to determine whether the ICWs propagated throughout the nephrocyte cytoplasm, or within restricted cellular compartments, e.g. the cortical region of the nephrocyte. This will be an important question to resolve because in other cell types, the locality of the ICW indicates which subcellular functions depend on the calcium signal (reviewed for neurons in (Ross, 2012). Whilst pericardial nephrocytes are single celled with no direct cell-cell communication they are all exposed to the same haemolymph. If soluble factors that either inhibit or promote calcium signalling exist in the haemolymph, the asynchronicity observed *in vivo* suggests that other criteria within individual nephrocytes must first be met before an ICW is initiated. The *in vivo* findings therefore indicate that nephrocytes behave independently of each other, at least in terms of their endogenous calcium signalling.

In the dissected preparations it was observed that a synchronous

increase in nephrocyte calcium occurred when nephrocytes were prepared either in the presence of calcium-containing buffers, or when calcium was added to nephrocytes after dissection in calcium-free buffer. This signal dissipated over a period of ~40–60 s, with follow-on asynchronous ICWs similar to those seen *in vivo* within larval pericardial nephrocytes. Whilst it is unclear why dissection triggers the opening of cell surface calcium channels, it was possible, using EGTA to chelate extracellular calcium, to demonstrate that the GCaMP6 signal required an influx of calcium into the nephrocyte cytoplasm from the extracellular environment. Additionally, the GCaMP6 signal was significantly reduced in the presence of 2-APB, supporting the possibility that calcium entry occurred via *Orai* channels, opened as a consequence of store operated calcium entry (SOCE). To confirm this, *Stim* and *Orai* were silenced in nephrocytes, leading to abolition of the GCaMP6 signal, consistent with the calcium influx being a consequence of SOCE.

Albumin binding and endocytic uptake assays were used to explore whether SOCE was linked with nephrocyte function. The data indicated that albumin binding was equivalent regardless of whether extracellular calcium was present or had been chelated by EGTA. However, pre-treatment of nephrocytes for one hour with calcium-free buffer, EGTA or 2-APB led to a significant reduction to the amount of albumin that could bind nephrocytes. These data indicate that whilst initial binding of albumin to nephrocytes appears to be calcium independent, an influx of

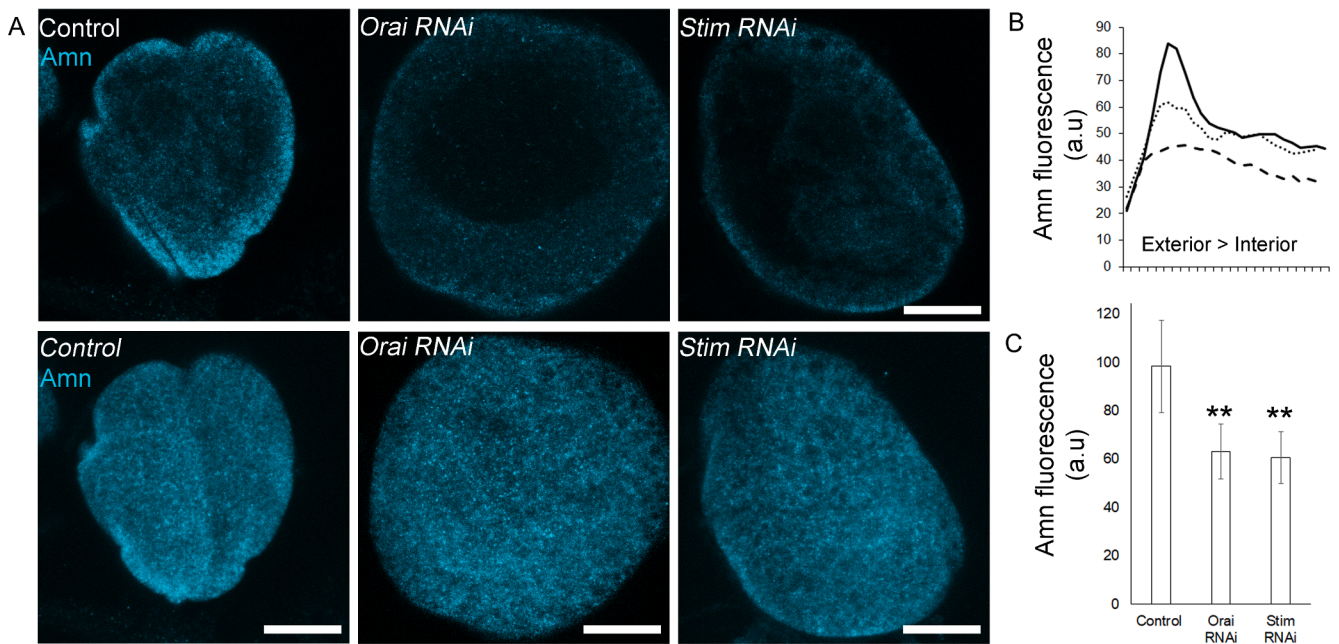


**Fig. 6.** Silencing *Orai* or *Stim* leads to abnormal distribution of Amnionless in nephrocytes. (A) Confocal micrographs of pericardial nephrocytes where *Orai* or *Stim* were silenced under the control of *Dot-Gal4* (control is *w<sup>1118</sup>* outcrossed to the *Dot-Gal4* driver line) that were stained with antibodies to Amnionless. Upper panels show single confocal slice through the midpoint of a single nephrocyte, the lower panels show z-projection of confocal stack through a single nephrocyte; scale bars = 15 μm. (B) Graph shows the profile of the Amnionless fluorescence signal over the nephrocyte surface; Control = solid line, *Orai RNAi* = dotted line, *Stim RNAi* = dashed line. (C) The graph shows quantified mean data for pericardial nephrocyte Amnionless signal in flies of the different genotypes; n = 22–30 nephrocytes from four different individual flies; \*\*\*P < 0.01 compared to control.

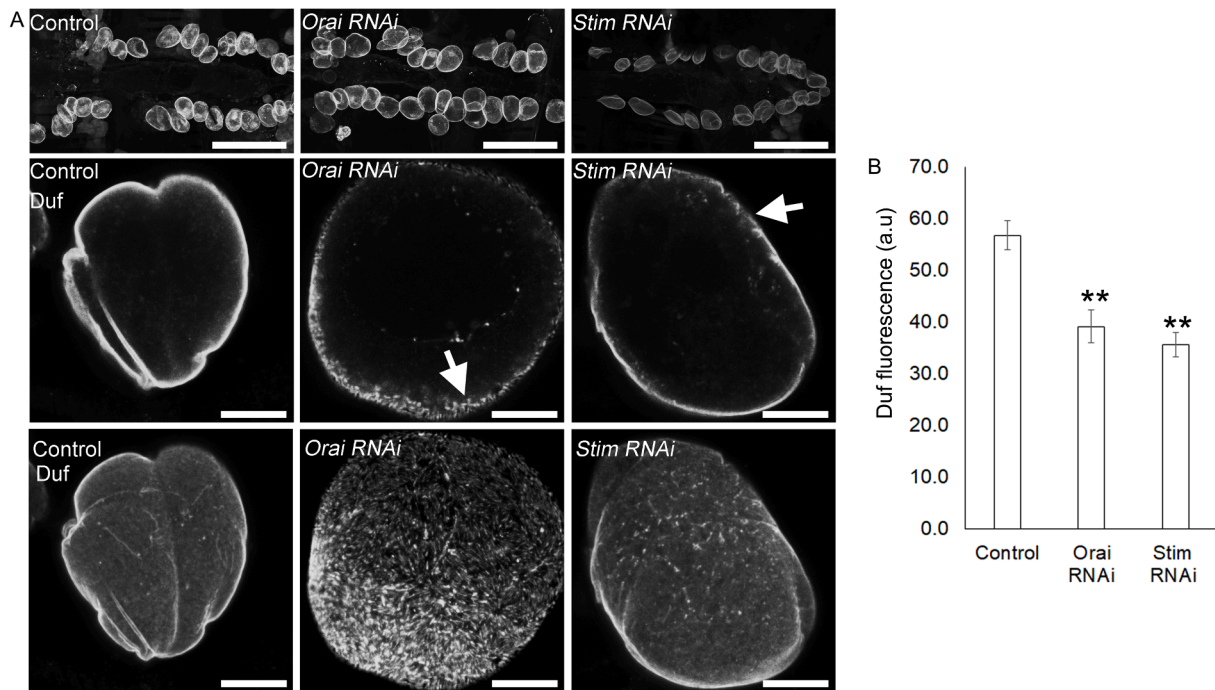


**Fig. 7.** Silencing *Orai* or *Stim* leads to abnormal distribution of Dumbfounded in nephrocytes. (A) Confocal micrographs of pericardial nephrocytes (the same cells that appear in Fig. 6) where *Orai* or *Stim* were silenced under the control of *Dot-Gal4* (control is *w<sup>1118</sup>* outcrossed to the *Dot-Gal4* driver line) that were stained with antibodies to the slit diaphragm protein Dumbfounded (Duf). Upper panels show single confocal stack through the midpoint of a single nephrocyte, the lower panels show z-projections of the entire nephrocyte. (B) The graph shows quantified data for Duf signal at the nephrocyte surface in flies of the stated genotypes; n = 20 nephrocytes from four different individual flies; \*\*\*P < 0.01 compared to control.

extracellular calcium is required over time to maintain albumin binding sites at the nephrocyte surface. Given that reduced albumin binding and an accumulation of Amnionless were observed within one hour of EGTA

or 2-APB treatment, the rate of Amnionless turnover appears very high, consistent with its extremely high level of gene expression in nephrocytes (Leader et al., 2018). In contrast, the slit diaphragm protein

Dumbfounded appeared to be largely unaffected by these calcium-modulating pre-treatments, suggesting either that its localisation is largely calcium-independent or if it is calcium-dependent, the mechanism of turnover is far less rapid than that seen for Amnionless.

When endocytosis was allowed to proceed after binding in the presence of extracellular calcium, albumin accumulated within nephrocytes as small puncta, consistent with their endocytic trafficking to early endosomes. In contrast, in the absence of extracellular calcium, few puncta were observed, and the albumin signal remained within the cortex of the nephrocyte, delineating the nephrocyte's labyrinthine channels, which are deep invaginations of membrane linking the extracellular environment to the nephrocyte cortex. This finding indicates that an influx of extracellular calcium into the nephrocyte is required for the uptake of albumin from the labyrinthine channel across the nephrocyte plasma membrane. Nephrocytes are an excellent model for the study of endocytic trafficking and recent studies of Garland cells revealed the existence of a novel four subunit CORVET complex (mini-CORVET), which tethers early endosomes. Further studies using fluorescently tagged Rab-GTPases, as well as transmission electron microscopy, would help elucidate the calcium-dependent points in the endocytic pathway that control Amnionless turnover (Lőrincz et al., 2016). Interestingly, nephrocytes pre-treated with 2-APB showed the most severe endocytic phenotype, with the greatest decrease to the bound albumin signal compared to EGTA or calcium-free buffer. Whilst 2-APB is a well-known blocker of SOCE channels it is also known to modify the activity of other calcium channels (it can activate TRPV1-3, TRPA1, and TRPM6 and inactivate TRPM2, TRPM7, TRPC3, TRPC6, and TRPC7 (Singh et al., 2018)). Given that the activity of mammalian ORAI channels can be modified by various TRP channels (Saul et al., 2014), this result needs to be investigated further as it may represent an interaction between the *Drosophila* Orai channel and TRP channels that might be of relevance to renal function in mammals or endocytosis in general.

Our observations indicated that short term chemical or pharmacological disruption of calcium signals led to an accumulation of Amnionless within nephrocytes, especially at the cortex. However, long term silencing of either *Stim* or *Orai* led to an overall downregulation of Amnionless within nephrocytes. These apparently contradictory results might be explained by a model whereby the short-term trafficking of Amnionless to the nephrocytes' surface is dependent on an influx of extracellular calcium, most likely via activation of Orai channels, whereas long-term impairment of calcium signalling leads to reduced Amnionless levels. In both the short-term pharmacological disruption of calcium signalling and the long-term RNAi-mediated disruption of calcium signalling the binding of albumin was significantly reduced indicating that SOCE is required for nephrocyte function, most likely through a mechanism involving Amnionless.

This interpretation is consistent with the findings from mammalian models, in which Amnionless was demonstrated to be associated with ORAI channels in the basal plasma membrane of human proximal tubular epithelial cells (Zeng et al., 2017). Indeed, it has been suggested that Amnionless is directly associated with ORAI1 and directly activated by STIM1 (Zeng et al., 2017). Our findings therefore support the existence of a conserved mechanism of SOCE in receptor-mediated endocytosis in insect nephrocytes involving Amnionless.

In terms of insect physiology these results highlight the possibility that nephrocyte function may decline in wild insects as a consequence of ingesting any factors that modify calcium signalling. Nephrocytes, due to their filtration function, preferentially accumulate toxins and whilst this is extensively employed as a useful functional assay in experimental models (Weavers et al., 2009; Ivy et al., 2015), a theme is emerging that nephrocytes and the 'nephrocytic system' of important wild pollinators can become disrupted in areas of high pollution (Domingues et al., 2017; Abdalla et al., 2015). Therefore, it will be important to explore the nephrocyte's role in insect health from an ecotoxicological point of view aided by data from both invertebrate and vertebrate experimental

'cardio-renal' models which could be translated to wild insects.

In summary we demonstrate that nephrocytes initiate ICWs *in vivo*, that SOCE is required for maintaining the cells' filtration function and that the SOCE genes *Stim* and *Orai* link the generation of ICWs to the cells' endocytic function via Amnionless. These findings indicate that insect nephrocytes have a dynamic signalling capacity which has not previously been recognised.

## Declaration of Competing Interest

The authors declare that they have no known competing financial interests or personal relationships that could have appeared to influence the work reported in this paper.

## Data availability

Data will be made available on request.

## Appendix A. Supplementary data

Supplementary data to this article can be found online at <https://doi.org/10.1016/j.jinsphys.2022.104453>.

## References

- Abdalla FC, Domingues CE da C. Hepato-Nephrocytic System: A Novel Model of Biomarkers for Analysis of the Ecology of Stress in Environmental Biomonitoring. PLOS ONE. 2015 Jul 21;10(7):e0132349.
- Atienza-Manuel, A., Castillo-Mancho, V., De Renzis, S., Culi, J., Ruiz-Gómez, M., 2021. Endocytosis mediated by an atypical CUBAM complex modulates slit diaphragm dynamics in nephrocytes. *Development* 148 (22) dev199894.
- Burford, J.L., Villanueva, K., Lam, L., Riquier-Brisson, A., Hackl, M.J., Pippin, J., et al., 2014. Intravital imaging of podocyte calcium in glomerular injury and disease. *J Clin Invest.* 124 (5), 2050–2058.
- Chen, T.W., Wardill, T.J., Sun, Y., Pulver, S.R., Renninger, S.L., Baohan, A., et al., 2013. Ultra-sensitive fluorescent proteins for imaging neuronal activity. *Nature.* 499 (7458), 295–300.
- Crossley, A.C., 1972. The ultrastructure and function of pericardial cells and other nephrocytes in an insect: *Calliphora erythrocephala*. *Tissue Cell.* 4 (3), 529–560.
- Denholm, B., Skaer, H., 2009. Bringing together components of the fly renal system. *Curr Opin Genet Dev.* 19 (5), 526–532.
- Domingues, C.E.C., Abdalla, F.C., Balsamo, P.J., Pereira, B.V.R., de Hausen, M., Costa, A., et al., 2017. Thiamethoxam and picoxystrobin reduce the survival and overload the hepato-nephrocytic system of the Africanized honeybee. *Chemosphere.* 186, 994–1005.
- Gass, M.M., Borkowsky, S., Lotz, M.L., Siwek, R., Schröter, R., Nedvetsky, P., et al., 2022. PI(4,5)P2 controls slit diaphragm formation and endocytosis in *Drosophila* nephrocytes. *Cell Mol Life Sci.* 79 (5), 248.
- Hartley, P.S., Motamedchaboki, K., Bodmer, R., Ocorr, K., 2016. SPARC-Dependent Cardiomyopathy in *Drosophila*. *Circ Cardiovasc Genet.* 9 (2), 119–129.
- Helmstädter, M., Simons, M., 2017. Using *Drosophila* nephrocytes in genetic kidney disease. *Cell Tissue Res.* 369 (1), 119–126.
- Hurcombe, J.A., Hartley, P., Lay, A.C., Ni, L., Bedford, J.J., Leader, J.P., et al., 2019. Podocyte GSK3 is an evolutionarily conserved critical regulator of kidney function. *Nat Commun.* 10 (1), 403.
- Ivy, J.R., Drechsler, M., Catterson, J.H., Bodmer, R., Ocorr, K., Paululat, A., et al., 2015. Klf15 Is Critical for the Development and Differentiation of *Drosophila* Nephrocytes. *PLoS ONE.* 10 (8), e0134620.
- Jaffe, L.F., 2008. Calcium waves. *Philos Trans R Soc Lond B Biol Sci.* 363 (1495), 1311–1317.
- Jaffe, L.F., 2010. Fast calcium waves. *Cell Calcium.* 48 (2–3), 102–113.
- Johnson, J., Blackman, R., Gross, S., Soboloff, J., 2022. Control of STIM and Orai function by post-translational modifications. *Cell Calcium.* 103, 102544.
- Kowalevsky, A., 1886. Zum Verhalten des Rückengäßes und des gürlandenförmigen Zellenstrangs der Musciden während der Metamorphose (On the behavior of the dorsal vessels and the garland-shaped cell cord of the muscids during metamorphosis). *Biological Centralblatt.* 6, 74–79.
- Larsen, C., Etzerodt, A., Madsen, M., Skjold, K., Moestrup, S.K., Andersen, C.B.F., 2018. Structural assembly of the megadalton-sized receptor for intestinal vitamin B12 uptake and kidney protein reabsorption. *Nat Commun.* 9 (1), 5204.
- Leader DP, Krause SA, Pandit A, Davies SA, Dow JAT. FlyAtlas 2: a new version of the *Drosophila melanogaster* expression atlas with RNA-Seq, miRNA-Seq and sex-specific data. *Nucleic Acids Res.* 2018 Jan 4;46(Database issue):D809–15.
- Li, F., Yang, C., Yuan, F., Liao, D., Li, T., Guilak, F., et al., 2018. Dynamics and mechanisms of intracellular calcium waves elicited by tandem bubble-induced jetting flow. *Proc Natl Acad Sci U S A.* 115 (3), E353–E362.
- Lőrincz, P., Lakatos, T., Varga, Á., Maruzs, T., Simon-Vecsei, Z., Darula, Z., et al., 2016. MiniCORVET is a Vps8-containing early endosomal tether in *Drosophila*. *Elife.* 02, 5.

- Maywald, M.L., Picciotto, C., Lepa, C., Bertgen, L., Yousaf, F.S., Ricker, A., et al., 2022. Rap1 Activity Is Essential for Focal Adhesion and Slit Diaphragm Integrity. *Front Cell Dev Biol.* 18 (10), 790365.
- Nivala, M., Ko, C.Y., Nivala, M., Weiss, J.N., Qu, Z., 2013. The emergence of subcellular pacemaker sites for calcium waves and oscillations. *J Physiol.* 591 (Pt 21), 5305–5320.
- K. Ocorr M. Fink A. Cammarato S. Bernstein R. Bodmer Semi-automated Optical Heartbeat Analysis of small hearts *J Vis Exp.* 2009;(31).
- Ross, W.N., 2012. Understanding calcium waves and sparks in central neurons. *Nat Rev Neurosci.* 13 (3), 157–168.
- Ruiz-Gómez, M., Coutts, N., Price, A., Taylor, M.V., Bate, M., 2000. *Drosophila* Dumbfounded: A myoblast attractant essential for fusion. *Cell* 102 (2), 189–198.
- Saul, S., Stanisz, H., Backes, C.S., Schwarz, E.C., Hoth, M., 2014. How ORAI and TRP channels interfere with each other: interaction models and examples from the immune system and the skin. *Eur J Pharmacol.* 15 (739), 49–59.
- Schneider, C.A., Rasband, W.S., Eliceiri, K.W., 2012. NIH Image to ImageJ: 25 years of image analysis. *Nat. Methods* 9 (7), 671–675.
- Singh, A.K., Saotome, K., McGoldrick, L.L., Sobolevsky, A.I., 2018. Structural bases of TRP channel TRPV6 allosteric modulation by 2-APB. *Nat. Commun.* 9 (1), 2465.
- Szebényi K, Füredi A, Kolacsek O, Csohány R, Prókai J, Kis-Petik K, et al. Visualization of Calcium Dynamics in Kidney Proximal Tubules. *J Am Soc Nephrol.* 2015 Nov;26 (11):2731–40.
- Troha K, Nagy P, Pivovarov A, Lazzaro BP, Hartley PS, Buchon N. Nephrocytes Remove Microbiota-Derived Peptidoglycan from Systemic Circulation to Maintain Immune Homeostasis. *Immunity.* 2019 15;51(4):625-637.e3.
- Tutor, A.S., Prieto-Sánchez, S., Ruiz-Gómez, M., 2014. Src64B phosphorylates Dumbfounded and regulates slit diaphragm dynamics: *Drosophila* as a model to study nephropathies. *Development* 141 (2), 367–376.
- Weavers, H., Prieto-Sánchez, S., Grawe, F., Garcia-López, A., Artero, R., Wilsch-Bräuninger, M., et al., 2009. The insect nephrocyte is a podocyte-like cell with a filtration slit diaphragm. *Nature* 457 (7227), 322–326.
- Zeng, B., Chen, G.L., Garcia-Vaz, E., Bhandari, S., Daskoulidou, N., Berglund, L.M., et al., 2017. ORAI channels are critical for receptor-mediated endocytosis of albumin. *Nat Commun.* 8 (1), 1920.
- Zhuang, S., Shao, H., Guo, F., Trimble, R., Pearce, E., Abmayr, S.M., 2009. Sns and Kirre, the *Drosophila* orthologs of Neph1 and Neph2, direct adhesion, fusion and formation of a slit diaphragm-like structure in insect nephrocytes. *Development* 136 (14), 2335–2344.